HHS Public Access

Author manuscript

Lab Chip. Author manuscript; available in PMC 2020 August 07.

Published in final edited form as:

Lab Chip. 2019 August 07; 19(15): 2589–2597. doi:10.1039/c9lc00417c.

Polycaprolactone-enabled sealing and carbon composite electrode integration into electrochemical microfluidics

Kevin J. Klunder[a,b], **Kaylee Clark**[a], **Cynthia McCord**[a], **Kathleen E. Berg**[a], **Shelley D. Minteer**[b], **Charles S. Henry**[a,*]

[a]Department of Chemistry, Colorado State University, Fort Collins, CO 80523

[b]Department of Chemistry, University of Utah, Salt Lake City, UT 84112

Abstract

Combining electrochemistry with microfluidics is attractive for a wide array of applications including multiplexing, automation, and high-throughput screening. Electrochemical instrumentation also has the advantage of being low-cost and can enable high analyte sensitivity. For many electrochemical microfluidic applications, carbon electrodes are more desirable than noble metals because they are resistant to fouling, have high activity, and large electrochemical solvent windows. At present, fabrication of electrochemical microfluidic devices bearing integrated carbon electrodes remains a challenge. Here, a new system for integrating polycaprolactone (PCL) and carbon composite electrodes into microfluidics is presented. The PCL:carbon composites have excellent electrochemical activity towards a wide range of analytes as well as high electrical conductivity (~1000 S m^{-1}). The new system utilizes a laser cutter for fast, simple fabrication of microfluidics using PCL as a bonding layer. As a proof-of-concept application, oil-in-water and water-in-oil droplets are electrochemically analysed. Small-scale electrochemical organic synthesis for TEMPO mediated alcohol oxidation is also demonstrated.

Graphical Abstract

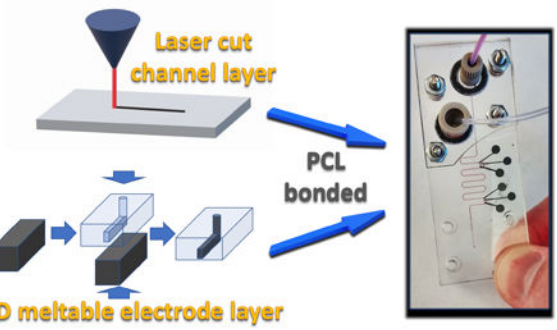

*Corresponding author.

†Footnotes relating to the title and/or authors should appear here.

Electronic Supplementary Information (ESI) available: [details of any supplementary information available should be included here]. See DOI: 10.1039/x0xx00000x

Conflicts of interest

There are no conflicts to declare.

Introduction

Electrochemistry coupled with microfluidics is an attractive platform to perform chemical analyses and/or chemical reactions with integrated detection. As such, electrochemical microfluidic devices have found use in biosensing, environmental monitoring, and point-of-care diagnostics.[1-4] Flow based electrochemistry is also highly desirable for electrochemical synthesis which has seen a significant amount of interest recently.[5, 6] While it is highly desirable to couple electrodes with a microfluidic chip, in practice, these devices can be difficult to manufacture. Metallic electrodes made from platinum or gold are often used but typically require expensive fabrication methods and the need for sophisticated cleanroom space.[3] In addition, the metal electrodes are not fully integrated into the substrate and often have raised features, meaning that sealing a channel over them can be challenging. Finally, precious metal electrodes can be prone to fouling.[7] An attractive alternative to noble metals are carbon composite electrodes, which are low cost, less prone to fouling, and enable sensing moieties and/or catalyst integration directly into the electrode.[8–10]

Unfortunately, carbon electrodes are also difficult to integrate into electrochemical microfluidics because they also have raised features,[11–13] require elaborate micromolding techniques with harsh chemicals,[14, 15] and/or require insertion into the device after the microfluidic is sealed.[16] There are a few examples of integrated epoxy-based carbon electrodes in microfluidics, but they need to be mixed and cast into a template quickly to allow generation of the correct geometry.[17–19] The difficulty of integrating carbon electrodes has led researchers to place electrodes in the waste area where sample dispersion and therefore, signal decrease occurs.[20] While pyrolysis can create exquisite μm-featured carbon electrodes with favourable conductivity and electrochemical activity,[21, 22] the high temperatures required make the integration into common polymer-based microfluidics impossible.[23] Poly(dimethylsiloxane) (PDMS)-based devices are also known but suffer from low conductivity and apparent diminished electrochemical activity.[24]

The main thrust of the work presented herein is to overcome tedious methods and high-cost materials for the integration of carbon electrodes into microfluidics. To achieve this goal, polycaprolactone (PCL) was used as a novel binder material for creating carbon composite electrodes. PCL composite electrodes for electrochemical applications have not been demonstrated previously, despite PCL having nearly ideal properties for making composite electrodes. PCL melts at 56–65 °C,[25] is soluble in common organic solvents, is inexpensive, and is readily available. PCL is also approved by the FDA for use in drug delivery, prosthetics, and medical applications providing the long-term potential for integration as wearable devices.[26, 27]

Herein we report the first use of PCL carbon composite electrodes and their integration into microfluidic devices. The electrochemistry of the new PCL:carbon composites was characterized first. Four different carbon particle types were tested with differing ratios of PCL:carbon to find an ideal composite. Following electrochemical characterization, microfluidic devices were fabricated using a CO_2 laser and sealed using PCL as a bonding layer. Finally, as a proof-of-concept, an electrochemical droplet generator, as well as a bulk electrolysis micro-reactor, are demonstrated. As a whole, the work presented here represents

a new strategy to easily assemble low-cost, high-end microfluidics with embedded carbon composites for enhanced electrochemical detection.

Results and Discussion

Fabrication of PCL electrodes.

Fabricating microfluidics with integrated electrodes requires patterning the electrode material onto or into a substrate. Patterned PCL and graphite electrodes were assembled, as shown in Figure 1. The process is simple and begins with dissolving PCL in dichloromethane (DCM) followed by mixing graphite powder with the dissolved plastic. The graphite, solvent, and plastic mixture is then poured onto a non-stick surface (Si wafer for example) and mixed until it becomes a semi-solid. Finally, the material is allowed to fully dry in a fume hood. Once solvent free, the material can be stored for later use. The dried material can also be shaped or ground up and stored as a powder, pellets, sheets, or blocks. We found no change in the materials properties after 6 months of storage in a glass vial at ambient conditions.

To make patterned electrodes, the dried composite is heated above the melting point of PCL to 70–85 ^{O}C, and then pressed into templates. Any technique which delivers pressure and heat could be used to make the electrodes, such as a hot plate and large weight, or clamps and an oven. In this work, a traditional hydraulic heated press was used. Once cooled, the excess material is carved off the surface with a razor blade, followed by smoothing the surface with sandpaper. Furthermore, a wide range of templates could likely be used in the future, ranging from laser cut structures in plastic to glass or metal forms. Here, laser cut poly(methyl methacrylate) (PMMA) structures containing defined patterns were used as templates. As shown in Figure 1, the electrodes can also be patterned in 3 dimensions, which allows for a well-defined electrode area and the ability to make easy electrical contact from the backside to a given piece of instrumentation.

We next considered the electrode roughness, since it could impact the fabrication of microfluidic devices. The roughness of the electrode/substrate was dependent on the type of sandpaper used to remove the excess electrode material. Upon polishing/sanding with a fine 3000 grit sandpaper, the electrode roughness was estimated to be ≤1 μm as determined by optical profilometry with 1 μm height resolution. A smooth, well-integrated surface is important for sealing microfluidics and is a major advantage of this new fabrication method.

Figure 1 also contains an SEM image of a PCL composite electrode. A high density of exposed graphitic flakes can be seen. The surface at the nm-scale is heterogeneous, containing bent/folded and randomly oriented graphitic domains. At higher magnification, numerous exposed graphitic edge sites are clearly present. Edge plane graphite is reportedly the most electrochemically active, and the high density of these sites on the PCL composites should be favourable for performing electrochemical measurements.[28] SEM Images for the other carbon types can be found in Figure S1–S3. In general, the various graphites had similar surface structure, except carbon black, which appeared to be composed of small nm-sized spherical particles.

Conductivity and capacitance.

Conductivity and capacitance are important for electrode performance. Highly resistive electrodes can cause ohmic drop in an electrochemical cell and lead to errors in applied potential,[29] while large capacitance values increase background signal. Four carbons were chosen from various commercial sources and tested at various ratios of binder to graphite to understand the impact on conductivity and capacitance. The methods section contains information on the supplier and the particle size. The results of the study are shown in Figure 2. As expected, conductivity increases with increasing carbon content. Below ~40 S m^{-1}, an electrode has undesirable resistance for use in a microfluidic device, and any composition that had a value below this was considered unusable. The conductivity values near the 1:2 ratio for most of the graphitic carbons are above this value. The carbon black electrode could not support more than a 1:1 ratio without losing mechanical stability. In general, the conductivity values and trends are similar to other high-end composite materials.[30]

The electrodes have higher capacitance than planar graphite electrodes; basal and edge plane graphitic electrodes have capacitance values of ≤2 and ~60 μF cm^{-2}, respectively.[31] The PCL-based composites had capacitance values in the range of 200 to 1000 μF cm^{-2}. This implies that the PCL composites have at least 3x the surface area than flat graphitic electrodes, which is reasonable considering the heterogeneity observed in the SEM images. When taken as a whole the ratio near 1:2 has the best balance of low capacitance and favourable conductivity. Also, the melt processing fabrication method is typically easier with increased PCL content. Given the results in Figure 2, the MG-1599, 3569, and 11 μm graphites at high and low ratios were chosen for further electrochemical analysis. Carbon black was not studied further as it had increased capacitance at lower ratios as well as a lower overall conductivity.

Electrochemical characterization.

The electrochemical activity of the new PCL carbon composites was characterized next. The goal was to elucidate if one carbon is more active than another and how the ratio of carbon affects the electrochemistry. The redox species chosen are commonly used for electrode activity quantification (ferricyanide and ferrocene) and biological molecules often used for lab-on-a-chip applications (ascorbic acid, p-aminophenol, uric acid, and benzoquinone).[31–33]

Initially, the electrodes were examined with ferricyanide and ferrocene-trimethylamine ($FcTMA^+$). These molecules typically have fast kinetics, and in the case of ferricyanide, charge transfer rate constants are known for a variety of carbon electrodes. The rate constant is a gauge of the electrochemical activity of the electrodes and can be used as a comparison between carbon materials. Cyclic voltammograms for $FcTMA^+$ can be found in the SI (Figure S4), as well as a details on the methods used to determine the rate constants. Attempts to calculate the rate constants for $FcTMA^+$ were performed; however, the electrodes were too active to measure kinetics with traditional methods (see SI for details).

The table in Figure 3 lists the electrochemical rate constant k^o for a variety of electrode compositions towards ferricyanide. Interestingly, the rate constants are similar between high and low ratios of carbon, except in the case of the larger particle size 3569-based composite where the rate constant is 2x larger for the higher ratio. Recently, a report relating graphite particle size and electrochemical activity claimed that larger particles are less active due to a decrease in edge plane graphite.[34] Perhaps the 3569 particles are also have a decrease in active edge plane sites. Overall, the rate constants are consistent with polished glassy carbon surfaces (0.005 cm s^{-1}).[31] The similar rate constants to traditional carbon electrodes is an encouraging result and imply that these electrodes will have broad utility when embedded into microfluidic devices. To balance fabrication simplicity with favourable electrochemistry, the 1:2 PCL:carbon ratio was chosen for analysis of biologically relevant redox species.

The data for biologically relevant redox molecules is shown in Figure 3. For the oxidation of ascorbic acid (AA), the different carbons gave similar electrochemistry. The onset potentials for AA oxidation are about −0.05 V vs. SCE and similar to that of a carbon nanotube and an electrochemically pre-treated carbon electrode.[35] The low onset potential is also indicative of a highly active electrode surface. The biggest discrepancy in AA oxidation was with the 3569 particles, where a lower peak current and a peak shift to higher potentials was seen.

Uric acid oxidation for all three carbons occurred at 0.3 V vs. SCE which is similar to a report using graphene, with glassy carbon having a peak at 0.4 V vs. SCE.[36] Related, the activity of the PCL composites was similar to a glassy carbon electrode in a buffered solution for the electrochemical reduction of 1,4-benzoquinone.[37] p-Aminophenol oxidation can often be difficult, however, the PCL composites gave well defined and reversible peaks that are similar to a highly active reduced graphene electrode.[38] Overall, the PCL graphite composites show responses akin to more exotic carbon materials such as carbon nanotubes or graphene. In a previous work which utilized PMMA and graphite, it was proposed that sanding activated and exfoliated the graphitic flakes. It is the polishing/sanding with 3000 grit sandpaper which appears to expose freshly cleaved graphite and create a highly active electrode material, perhaps a similar activation is happening here with the PCL composites.[30]

Fabrication of PCL sealed microfluidics with integrated electrodes.

Following the electrochemical characterization of the composites, 1:2 PCL:MG-1599 was chosen for integration into microfluidic devices. The 1:2 ratio allows for a significant percentage of PCL within the composite, which may help with sealing the electrodes within devices. It was also observed that lower ratios of PCL:carbon flowed into templates easier than higher ratios, simplifying fabrication. PMMA was chosen as a base material to fabricate microfluidics, PMMA is reported to be one of the best for use with a CO_2 laser engraver/cutter in regards to the quality of cut.[39–42]

Sealing PMMA-based microfluidics can be done with a variety of techniques,[43] including thermal bonding,[44] plasma treatment,[45] plastisizers,[46] microwave treatment,[47] ultrasonic assisted bonding,[48] or solvent bonding.[49, 50] Another common technique is to apply a thin adhesive layer to join the two halves.[51, 52] As an alternative to the previously mentioned

methods, the devices assembled here were sealed by applying a thin layer of PCL. PCL has a lower melting temperature than PMMA and, when heated under pressure, can bond two pieces without deforming the PMMA.[53] There is currently only a single report on the use of PCL as a sealing layer, as reported by the Remcho group.[54] The optimum conditions in that work were spin coating a 3% w/v PCL solution onto a substrate. To make the coating process easier and eliminate the need for specialized equipment, we developed a “push coating” method. Push coating appears to be a new concept for assembling microfluidics, but has been previously used for creating patterned thin film transistors.[55]

Figure 4 shows the process for the fabrication of PCL sealed devices. Initially, a small amount of PCL:DCM solution was placed onto a silicon wafer. Next, a blank PMMA slide was firmly pressed by hand onto the PCL:DCM bead of solution. The amount of PCL:DCM solution used was in excess so that it squeezes out on all sides of the PMMA plate. Finally, we found the optimal PCL:DCM ratio to be 1:100 by mass, which provided a coating thickness of 3 ± 1 μm (n=9). When the PCL:DCM ratio was less than 1:100, the PMMA/PCL stuck to the silicon wafer, making removal difficult.

After the PCL film was applied to the blank piece of PMMA, the microfluidic channel was generated with a CO_2 laser operating in raster mode. The process is shown in the middle of Figure 4. In contrast to previous PCL-sealed microfluidics,[54] the channel was cut into the plate containing the PCL film. Channel dimension are defined by the optics of the laser cutter and typical channel dimensions were 150 μm deep and 300 μm wide. Channels ablated in the x-axis are triangular in shape and are 40 μm wide near the bottom of the triangle (Figure S6).

In terms of reproducibility, a report using a laser from the same manufacture used here reported a batch to batch variance in cut quality of 15%, the work also highlights strategies to obtain optimal cut quality.[56] While channels cut with a laser cutter often have some roughness (Fig. S6 & S7), if desired there are relatively simply strategies to significantly smooth them.[57] Overall, it was not the main thrust of this work to achieve ultra-high precision of channel and electrode dimensions, however, the same fabrication strategy could be used with high resolution embossed pieces. Indeed, the use of the PCL bonding layer is highly advantageous to maintain channel resolution as PCL has a ~60 °C lower melting point than that of PMMA.[54]

Sealing the device is rapid and involves placing the two halves in a heated press at 85 ^{O}C for 5 min. Chips could also be made by placing the pieces between clamps followed by heating in an oven (85 ^{O}C). It was found to be critical to cool the chip under pressure to maintain the seal. Occasionally a device would only partially seal depending on the complexity of the design and size of the device. In those cases the sealing process (heat and pressure/cooling and pressure) was repeated until a fully sealed device was obtained. It was also discovered that the electrode layer was reusable many times over. Heating the chip above 70 °C and prying apart the layers, followed by sanding the surface, provided an electrode layer that was fully reusable.

Electrochemistry of PCL composites in a droplet generator.

The electrochemistry of droplets dates back to 2008, in which the first report used the technique to determine the frequency, droplet size, and droplet velocity.[58] Following this work, only a handful of examples of electrochemistry in droplets within microfluidic devices exist.[59–64] The limited number of reports probing the redox behaviour within droplets is likely the result of the oil/water systems used to create droplets. The oil phase is non-conductive and can deactivate the electrode surface by coating it with an insulating layer.[64] As a whole, this challenging system is ideal for testing the activity and durability of the PCL:graphite-based electrochemical microfluidics.

There are many different configurations for microfluidic droplet generators,[65] in this work, a pinching droplet generator was selected. Figure 5 shows water-in-oil as well as oil-in-droplets being generated. PMMA is not sufficiently hydrophobic to create water-in-oil droplets so the channels were silanized, as previously reported.[66] While it was possible to generate water-in-oil droplets (Figure 5A), sensing of ferricyanide contained within the droplets was found to be difficult and lacked reproducibility. Example chronoamperometry results for the sensing of ferricyanide in water droplets (Figures S8 and S9) and related videos are provided in the SI. Stable droplets were generated for short periods of time but, in general, droplet generation was not stable enough for consistent electrochemistry.

The devices used to generate oil-in-water droplets required no pre-treatment of the PMMA surface. Oil droplets separated by aqueous plugs were readily formed, and the electrochemical data is shown in Figure 5B. Video of the droplet formation is shown in the SI. The device used 3 inlets and was capable of changing the flow rate of a blank electrolyte solution, a solution containing analyte, and the oil phase. The total flow rate of the oil and the aqueous phase was kept a constant 8 μL min^{-1} for the aqueous phase and 2 μL min^{-1} for the oil phase. By varying the flow rate of the two aqueous streams, the concentration of the analyte could be adjusted. The dilution factor, ratio of electrolyte:ferricyanide, are shown in the right hand side of the top graph in Figure 5B. Figure 5B also shows that as the concentration increases there is an increase in both the peak height as well as the total observed current. The currents were plotted for peak height and total current maximum (Figure 5D). Both results show a linear response as a function of concentration. A linear relationship is expected, since current is linearly related to concentration in a laminar flow cell at a band electrode confined within a channel.[22] It is interesting that the current does not approach zero when an oil droplet passes over the electrode, this implies that the electrode remains in contact with the aqueous phase at all times. It is logical that a thin layer of aqueous solution is always in contact with the electrode since this is a requirement for stable oil droplets.

Electrochemistry of PCL composites in a micro-electrochemical reactor.

For a final demonstration of the PCL-based electrochemical microfluidic system, a chip was created for small-scale electrochemical organic synthesis. Organic electrochemical synthesis is reportedly on the verge of a renaissance, due in part to the ability of electrochemistry to replace hazardous oxidants or reductants.[67–69] By replacing harsh reagents with an

electrode, it allows chemists to simplify previously difficult, costly, and/or inaccessible chemical reactions.[70]

The PMMA used to create microfluidics here was not compatible with organic solvents, so aqueous systems were used. PMMA is reportedly stable under acidic and basic conditions which means a wide range of reactions are accessible for the PCL/PMMA-based devices. One reaction performed under aqueous conditions that is gaining attention for electrochemical applications is TEMPO-mediated alcohol oxidation, and recently TEMPO was proposed for use in commercial chemical synthesis.[71]

Here, the reactor was initially characterized by flowing 4-methoxy-TEMPO through the cell and monitoring the steady state current as a function of potential. Figure 6A shows that as the potential is increased there is a clear steady state response from TEMPO over the blank. At near 1.1 V vs. carbon, the PCL:graphite electrode appears to start the oxidation of either the carbon surface or the solvent. The data in Figure 6A was used to elucidate the optimal voltage for electrolysis, which was determined to be 0.9 V vs. carbon.

Oxidation of piperonyl alcohol was then attempted in the flow cell. The device has a small mixing area shown in Figure 6C followed by electrolysis zones. The flow rates were adjusted in real-time until a current response near the theoretical amount needed for full conversion was obtained. This rate was 2 μL min^{-1} for the substrate and 3 μL min^{-1} of TEMPO. The ability to adjust flow rates in real time is a unique aspect to microfluidics for improving product yields in real time based on current. The increased current over what is theoretically predicted for full electrolysis may be from redox cycling of the TEMPO as it passes from the working to the counter electrode. The steady state current in Figure 6B at 0.9 V vs. carbon is about 4x lower than with just TEMPO and no substrate (Figure 6A). The lower current may be related to a decrease in redox cycling as the TEMPO can now react with the substrate.

The reaction mixture was collected via the O-ring sealed exit port, and once 1.8 mL was recovered, the eluent was extracted with DCM and analysed by gas-chromatography mass spectrometry (GC-MS). It was found that there was full conversion to the aldehyde, determined by the lack of a peak near 8.3 min in the GC-MS chromatogram where the alcohol is detected. A modest yield of 43 % was also found. It is possible that some of the substrate was adsorbed by the PMMA and/or that the DCM extraction method was not entirely efficient. While high yields were not obtained, the experiment demonstrates that the electrodes could be used for prolonged electrolysis. The data also demonstrates that the new PCL-based electrochemical microfluidics have potential utility for small scale electrolysis experiments.

Conclusions

In conclusion, PCL has enabled the integration of carbon composite electrodes into complex microfluidics through a simple melt-based process. PCL coupled with a CO_2 laser cutter has also enabled a fast and highly robust assembly of the microfluidic devices. The techniques proposed enable quickly prototyping new electrochemical microfluidic designs. The new

PCL:carbon composites maintained prolonged electrochemical activity in diverse electrochemical microfluidic systems. Given the ease of making highly active μm-patterned electrodes, this work has significant impact for a wide range of fields relating to electroanalytical chemistry, or other applications requiring small, well-integrated electrodes placed within microfluidic devices.

Experimental methods

Reagents

The PCL was purchased from Amazon and was labelled ThermoMorph. ^{1}H-NMR characterization of Thermorph was performed to ensure that it was polycaprolactone, the data is located in the SI. All other reagents were from commercial chemical suppliers and used without further purification. Water was supplied by a 18.2 MΩ·cm water from a MilliPore (Billerica, MA, USA) Milli-Q system. The carbon was MG-1599 from Great Lakes Graphite, Inc. (size ~15 μm), 7–11 micron graphite from Fisher Scientific (size 7–11 μm), 3569 from Asbury Carbon (<150 μm), carbon black from STREM Chemicals, Inc. (~50 nm).

Conductivity and Capacitance measurements

Through-plane conductivity measurements were performed measuring resistance with a two-point probe (Fluke 187 multimeter, accuracy of 0.01 Ω) following the method previously reported.[30] The capacitance was measured with cyclic voltammetry in 0.5 M KNO_3 using the current response at 0.2 V vs. following the method previously reported.[30] In this work 2.5 mm disk of the composite that were normally 3 mm thick were used.

Electrochemistry

For 3-electrode voltammetry, the electrochemistry was performed with a CH Instruments 660b. An SCE reference was used for all experiments. The counter electrode was a composite plate of graphite, typically with a minimum of 10x the working area of the working electrode.

Flow cell experiments used PCL:Carbon in the same composition as the working electrode as the counter and reference. The electrolyte for droplet generation was 0.5 M KCl with 1% Tween20 surfactant, and light weight mineral oil. The voltage was held at −0.4 V vs. carbon.

Electrolysis experiments were performed in 0.3 M Na_2CO_3 at pH 10, 18.5 mM piperonyl alcohol and 10.6 mM 4-methoxy-TEMPO. Flow rate for each solution was 2.5 μL min^{-1}, 5 μL min^{-1} total. The buffer and 4-methoxy calibration curve was made with a flow rate of 5 μL min^{-1} and 10.6 mM of 4-methoxy-TEMPO.

Fabrication of microfluidics

For the push coating method, pressure was maintained for 1 min until the DCM was mostly evaporated. After 15 min, the plate was removed from the silicon wafer with a razorblade by scoring around the edges. After PCL coating the PMMA plate, an Epilog Zing (30 watt) with 25% speed and 30% power was used to create the channels. Connecting pumps to

microfluidic devices can be problematic.[37] Here, connections to the chips were made with a unique laser cut PMMA and O-ring detachable interface. The reusable connection pieces are labelled “interface layer” in Figure 4. PMMA was rastered (ablated) to accommodate an o-ring and then tapped to accept threaded standard microfluidic fittings. The interface layer is simply bolted to the sealed chip. The layer is quite robust and the screw fitting/ferrule can easily be coupled to the chip with a leak-less union.

Supplementary Material

Refer to Web version on PubMed Central for supplementary material.

Acknowledgements

This worked was supported by the National Science Foundation under CHE-1710222 to CSH and the Center for Synthetic Organic Electrochemistry for funding (CHE-1740656) to SDM. Additional support was provided from the National Institutes of Health through grant numbers ES024719 and OH010662.

References

1. Dincer C, Bruch R, Kling A, Dittrich PS and Urban GA, Trends in biotechnology, 2017, 35, 728–742. [PubMed: 28456344]
2. Sameenoi Y, Koehler K, Shapiro J, Boonsong K, Sun Y, Collett J, Volckens J. and Henry CS, J. Am. Chem. Soc, 2012, 134, 10562–10568. [PubMed: 22651886]
3. Rackus DG, Shamsi MH and Wheeler AR, Chemical Society Reviews, 2015, 44, 5320–5340. [PubMed: 25962356]
4. Kudr J, Zitka O, Klimanek M, Vrba R. and Adam V, Sensor. Actuat. B-Chem, 2017, 246, 578–590.
5. Pletcher D, Green RA and Brown RCD, Chemical Reviews, 2018, 118, 4573–4591. [PubMed: 28921969]
6. Folgueiras-Amador AA and Wirth T, Journal of Flow Chemistry, 2017, 7, 94–95.
7. Tujunen N, Kaivosoja E, Protopopova V, Valle-Delgado JJ, Österberg M, Koskinen J. and Laurila T, Materials Science and Engineering: C, 2015, 55, 70–78. [PubMed: 26117740]
8. Kuhnline CD, Gangel MG, Hulvey MK and Martin RS, Analyst, 2006, 131, 202–207. [PubMed: 16440083]
9. Villalba MM and Davis J, J. Solid State Electr, 2008, 12, 1245–1254.
10. Peltola E, Sainio S, Holt KB, Palomäki T, Koskinen J. and Laurila T, Anal. Chem, 2018, 90, 1408–1416. [PubMed: 29218983]
11. Hamedi MM, Unal B, Kerr E, Glavan AC, Fernandez-Abedul MT and Whitesides GM, Lab on a Chip, 2016, 16, 3885–3897. [PubMed: 27714038]
12. Pereira SV, Bertolino FA, Fernandez-Baldo MA, Messina GA, Salinas E, Sanz MI and Raba J, Analyst, 2011, 136, 4745–4751. [PubMed: 21984978]
13. Kovarik ML, Torrence NJ, Spence DM and Martin RS, Analyst, 2004, 129, 400–405. [PubMed: 15116230]
14. Moore CM, Minteer SD and Martin RS, Lab on a Chip, 2005, 5, 218–225. [PubMed: 15672138]
15. Chen C-H, Lin Y-T and Lin M-S, Anal. Chim. Acta, 2015, 874, 33–39. [PubMed: 25910443]
16. Erkal JL, Selimovic A, Gross BC, Lockwood SY, Walton EL, McNamara S, Martin RS and Spence DM, Lab on a chip, 2014, 14, 2023–2032. [PubMed: 24763966]
17. Selimovic A, Johnson AS, Kiss IZ and Martin RS, Electrophoresis, 2011, 32, 822–831. [PubMed: 21413031]
18. Johnson AS, Selimovic A. and Martin RS, Electrophoresis, 2011, 32, 3121–3128. [PubMed: 22038707]
19. Xu X. and Weber SG, J. Electroanal. Chem, 2009, 630, 75–80.

20. Wang J, Pumera M, Chatrathi MP, Escarpa A, Konrad R, Griebel A, Dörner W. and Löwe H, Electrophoresis, 2002, 23, 596–601. [PubMed: 11870771]
21. Martinez-Duarte R, Gorkin Iii RA, Abi-Samra K. and Madou MJ, Lab on a Chip, 2010, 10, 1030–1043. [PubMed: 20358111]
22. Dumitrescu I, Yancey DF and Crooks RM, Lab on a Chip, 2012, 12, 986–993. [PubMed: 22282034]
23. Fischer DJ, Vandaveer WR, Grigsby RJ and Lunte SM, Electroanal, 2005, 17, 1153–1159.
24. Sameenoi Y, Mensack MM, Boonsong K, Ewing R, Dungchai W, Chailapakul O, Cropek DM and Henry CS, Analyst, 2011, 136, 3177–3184. [PubMed: 21698305]
25. Labet M. and Thielemans W, Chemical Society Reviews, 2009, 38, 3484–3504. [PubMed: 20449064]
26. Malikmammadov E, Tanir TE, Kiziltay A, Hasirci V. and Hasirci N, Journal of Biomaterials Science, Polymer Edition, 2018, 29, 863–893. [PubMed: 29053081]
27. Woodruff MA and Hutmacher DW, Prog. Polym. Sci, 2010, 35, 1217–1256.
28. Lowe ER, Banks CE and Compton RG, Electroanal, 2005, 17, 1627–1634.
29. Aller Pellitero M, Guimerà A, Villa R. and del Campo FJ, The Journal of Physical Chemistry C, 2018, 122, 2596–2607.
30. Klunder KJ, Nilsson Z, Sambur JB and Henry CS, J. Am. Chem. Soc, 2017, 139, 12623–12631. [PubMed: 28797166]
31. McCreery RL, Chem. Rev, 2008, 108, 2646–2687. [PubMed: 18557655]
32. Asadian E, Ghalkhani M. and Shahrokhian S, Sensors and Actuators B: Chemical, 2019, 293, 183–209.
33. Niwa O, Xu Y, Halsall HB and Heineman WR, Analytical Chemistry, 1993, 65, 1559–1563. [PubMed: 8328672]
34. Slate AJ, Brownson DAC, Abo Dena AS, Smith GC, Whitehead KA and Banks CE, Phys. Chem. Chem. Phys, 2018, DOI: 10.1039/C8CP02196A.
35. Musameh M, Lawrence NS and Wang J, Electrochem. Commun, 2005, 7, 14–18.
36. Argüello J, Leidens VL, Magosso HA, Ramos RR and Gushikem Y, Electrochim. Acta, 2008, 54, 560–565.
37. Quan M, Sanchez D, Wasylkiw MF and Smith DK, J. Am. Chem. Soc, 2007, 129, 12847–12856. [PubMed: 17910453]
38. Vilian ATE, Veeramani V, Chen S-M, Madhu R, Huh YS and Han Y-K, Anal. Methods, 2015, 7, 5627–5634.
39. Davim JP, Barricas N, Conceição M. and Oliveira C, Journal of Materials Processing Technology, 2008, 198, 99–104.
40. Choudhury IA and Shirley S, Optics & Laser Technology, 2010, 42, 503–508.
41. Shashi P. and Subrata K, Journal of Micromechanics and Microengineering, 2015, 25, 035010.
42. Yuan D. and Das S, Journal of Applied Physics, 2007, 101, 024901.
43. Temiz Y, Lovchik RD, Kaigala GV and Delamarche E, Microelectronic Engineering, 2015, 132, 156–175.
44. Zhu X, Liu G, Guo Y. and Tian Y, Microsyst Technol, 2007, 13, 403–407.
45. Liu J, Qiao H, Liu C, Xu Z, Li Y. and Wang L, Sensor. Actuat. B-Chem, 2009, 141, 646–651.
46. Duan H, Zhang L. and Chen G, Journal of Chromatography A, 2010, 1217, 160–166. [PubMed: 19945714]
47. Toossi A, Moghadas H, Daneshmand M. and Sameoto D, Journal of Micromechanics and Microengineering, 2015, 25, 085008.
48. Luo Y, Zhang Z, Wang X. and Zheng Y, Microelectronic Engineering, 2010, 87, 2429–2436.
49. Arshya B, Alireza N. and Hossein K, Journal of Micromechanics and Microengineering, 2016, 26, 065017.
50. Gan Z, Zhang L. and Chen G, Electrophoresis, 2011, 32, 3319–3323. [PubMed: 22072551]
51. Tsao C-W and DeVoe D, Microfluid Nanofluid, 2009, 6, 1–16.
52. Wasay A. and Sameoto D, Lab on a Chip, 2015, 15, 2749–2753. [PubMed: 26016928]

53. Yu H, Chong ZZ, Tor SB, Liu E. and Loh NH, RSC Advances, 2015, 5, 8377–8388.
54. Myra TK, Jintana N, Yuanyuan W, Ryan TF and Vincent TR, Journal of Micromechanics and Microengineering, 2012, 22, 115030.
55. Ikawa M, Yamada T, Matsui H, Minemawari H, Tsutsumi J. y., Horii Y, Chikamatsu M, Azumi R, Kumai R. and Hasegawa T, Nature Communications, 2012, 3, 1176.
56. Gabriel EFM, Coltro WKT and Garcia CD, Electrophoresis, 2014, 35, NA-NA.
57. Wang ZK, Zheng HY, Lim RYH, Wang ZF and Lam YC, Journal of Micromechanics and Microengineering, 2011, 21, 095008.
58. Liu S, Gu Y, Le Roux RB, Matthews SM, Bratton D, Yunus K, Fisher AC and Huck WTS, Lab on a Chip, 2008, 8, 1937–1942. [PubMed: 18941696]
59. Wu C, Shah A, Ye H, Chen X, Ye J, Jiang H, Chen B, Wang X. and Yan H, Anal. Chim. Acta, 2015, 857, 39–45. [PubMed: 25604818]
60. Rattanarat P, Suea-Ngam A, Ruecha N, Siangproh W, Henry CS, Srisa-Art M. and Chailapakul O, Anal. Chim. Acta, 2016, 925, 51–60. [PubMed: 27188317]
61. Gu S, Lu Y, Ding Y, Li L, Song H, Wang J. and Wu Q, Biosens. Bioelectron, 2014, 55, 106–112. [PubMed: 24368227]
62. Lin X, Hu X, Bai Z, He Q, Chen H, Yan Y. and Ding Z, Anal. Chim. Acta, 2014, 828, 70–79. [PubMed: 24845817]
63. Abadie T, Sella C. and Thouin L, Electrochem. Commun, 2017, 80, 55–59.
64. Liu H. and Crooks RM, Lab on a Chip, 2013, 13, 1364–1370. [PubMed: 23386119]
65. Teh S-Y, Lin R, Hung L-H and Lee AP, Lab on a Chip, 2008, 8, 198–220. [PubMed: 18231657]
66. Subramanian B, Kim N, Lee W, Spivak DA, Nikitopoulos DE, McCarley RL and Soper SA, Langmuir, 2011, 27, 7949–7957. [PubMed: 21608975]
67. Yan M, Kawamata Y. and Baran PS, Chem. Rev, 2017, 117, 13230–13319. [PubMed: 28991454]
68. Möhle S, Zirbes M, Rodrigo E, Gieshoff T, Wiebe A. and Waldvogel SR, Angew. Chem. Int. Edit, 2018, 57, 6018–6041.
69. Laudadio G, Barmpoutsis E, Schotten C, Struik L, Govaerts S, Browne DL and Noël T, Journal of the American Chemical Society, 2019, 141, 5664–5668. [PubMed: 30905146]
70. Peters BK, Rodriguez KX, Reisberg SH, Beil SB, Hickey DP, Kawamata Y, Collins M, Starr J, Chen L, Udyavara S, Klunder K, Gorey TJ, Anderson SL, Neurock M, Minteer SD and Baran PS, Science, 2019, 363, 838–845. [PubMed: 30792297]
71. Ciriminna R, Ghahremani M, Karimi B. and Pagliaro M, ChemistryOpen, 2017, 6, 5–10. [PubMed: 28168142]

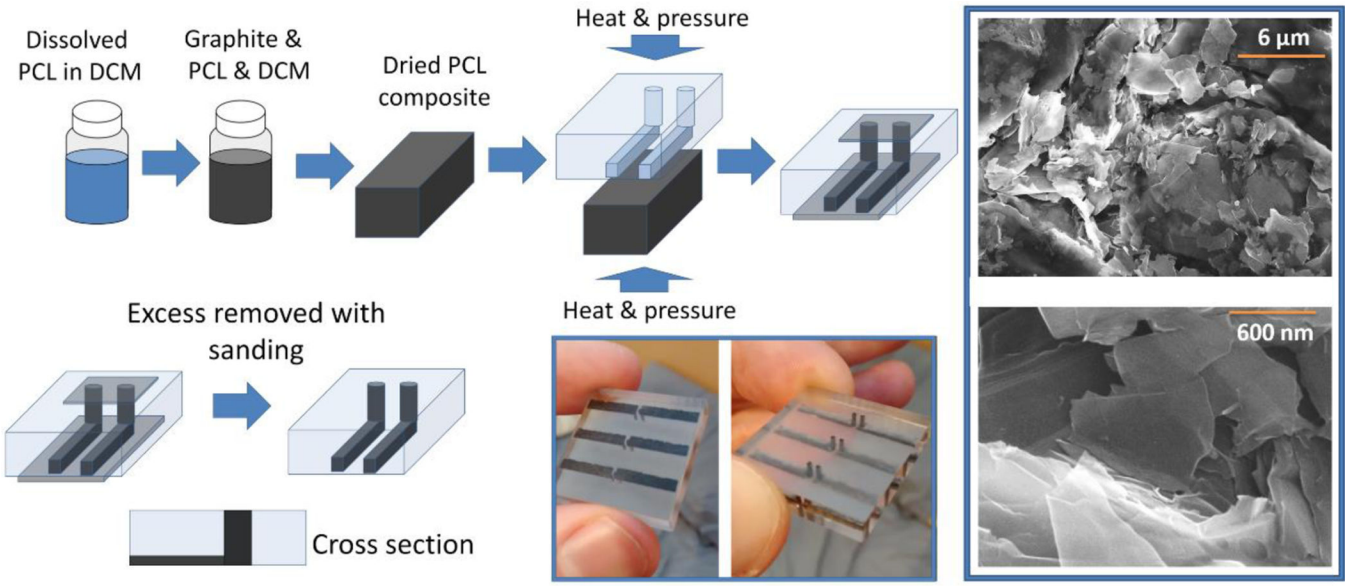

Figure 1.

CO_2 laser-enabled fabrication of 3-dimensional patterned PCL composite electrodes, and (right) SEM images at 5000x and 50,000x of a 1:2 MG PCL:carbon composite after sanding.

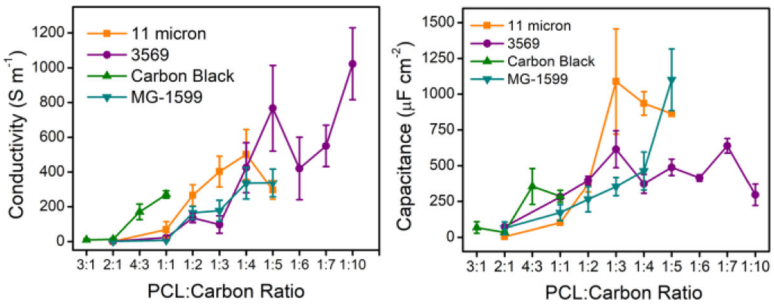

Figure 2.

Measured conductivity and capacitance values of various PCL:carbon ratios of different carbon types.

Electrode	1:2 PCL:carbon cm s^{-1}	1:4 PCL:carbon cm s^{-1}
3569	$0.0065 \pm 2x10^{-4}$	$0.0127 \pm 3x10^{-4}$
MG	$0.0083 \pm 3x10^{-4}$	$0.0085 \pm 3x10^{-4}$
11 μm	$0.0088 \pm 7x10^{-4}$	$0.0097 \pm 2x10^{-4}$

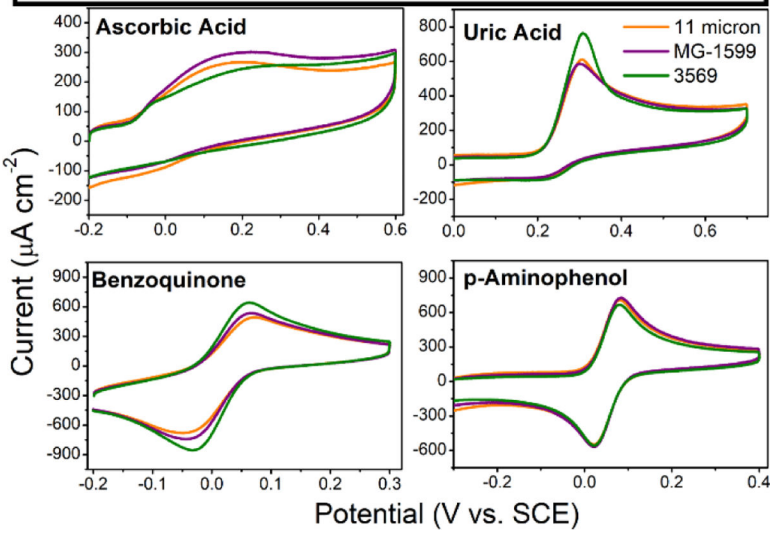

Figure 3.

(top) Table contains electrochemical rate constants of 5 mM ferri/ferrocyanide in 0.5 M KNO_3 in relation to differing electrode compositions. (bottom) Cyclic voltammetry of 1 mM substrate in 0.1 M phosphate buffer/pH 7.4, scan rate was 100 mV s^{-1}. All electrodes are in a 1:2 PCL:carbon ratio.

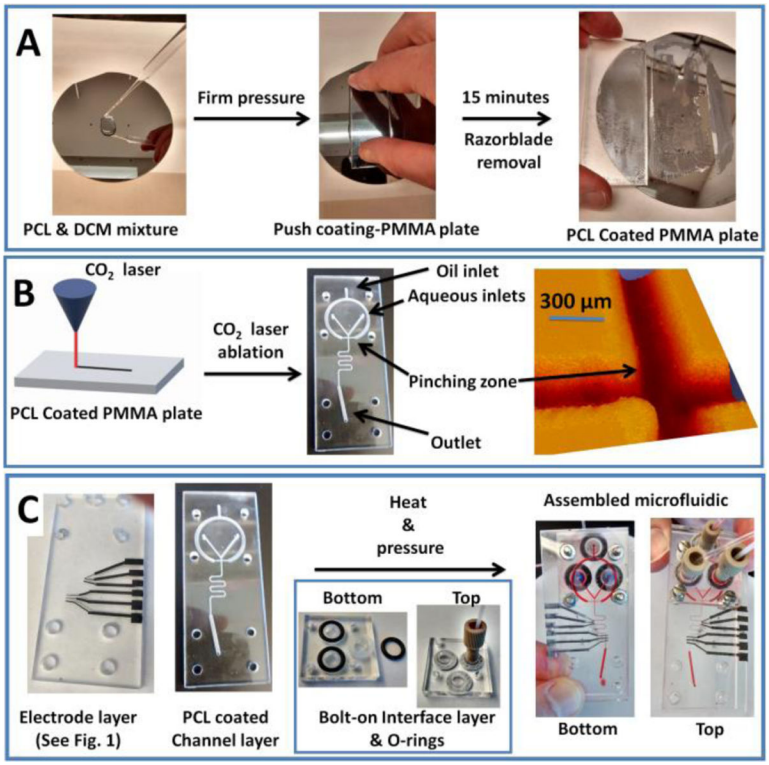

Figure 4.

(A) Method for creating a thin layer of PCL coated onto a PMMA plate. (B) Droplet generator design CO_2 laser engraved into a PCL coated PMMA plate. (C) PCL thin layer enabled bonding of the electrode and channel layers. The reusable bolt-on interface layer was mechanically tapped to accepted standard microfluidic screw fittings.

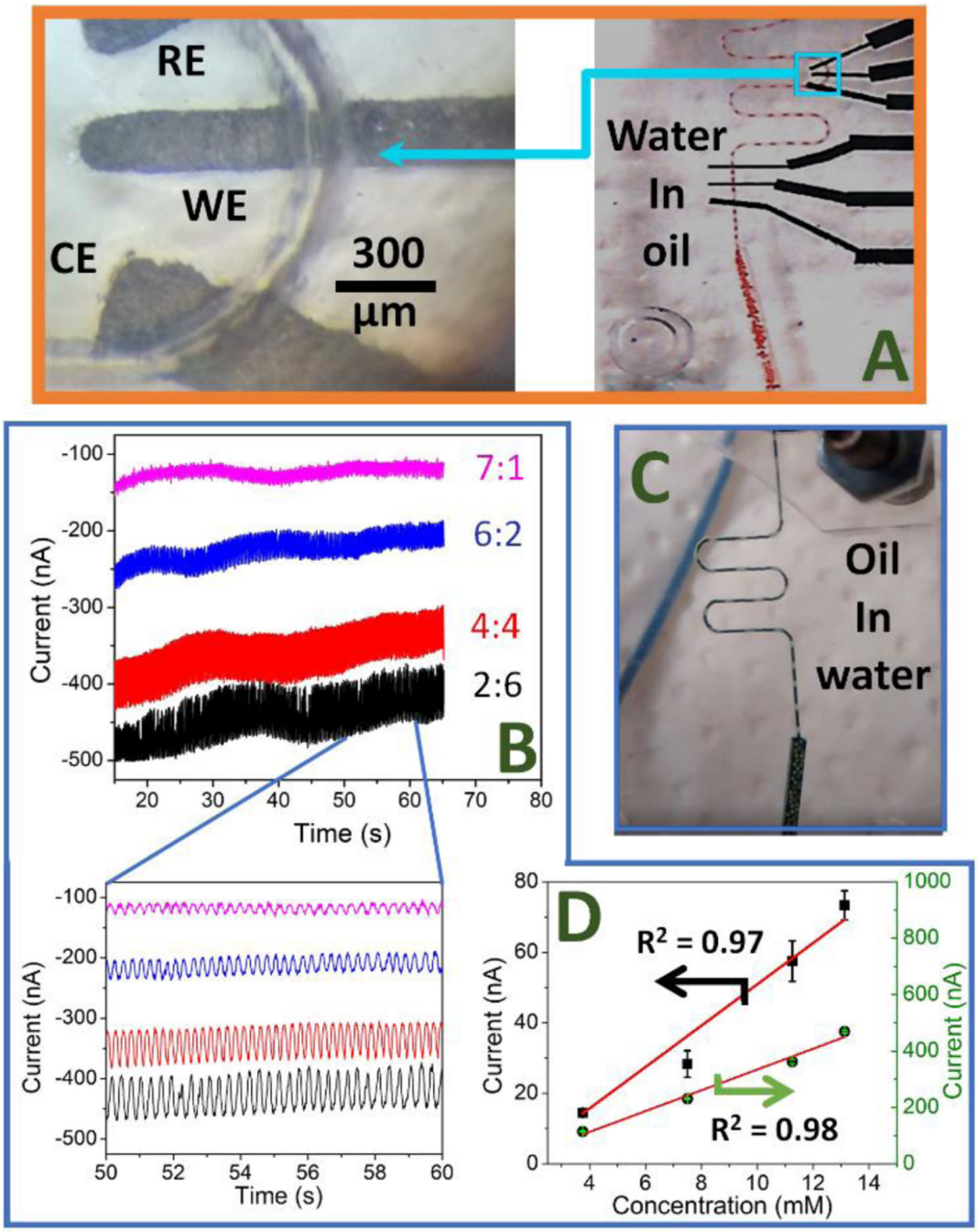

Figure 5.

(A) Image of electrodes interfaced to a channel in a sealed device and water-in-oil droplets doped with red dye. (B) Chronoamperometry of 15 mM ferricyanide solution at differing dilution ratios of electrolyte: analyte for oil-in-water droplets. (C) Photograph of oil-in-water droplets. (D) Peak height plotted as a function of concentration of ferricyanide. Arrows indicate the axes for each plot.

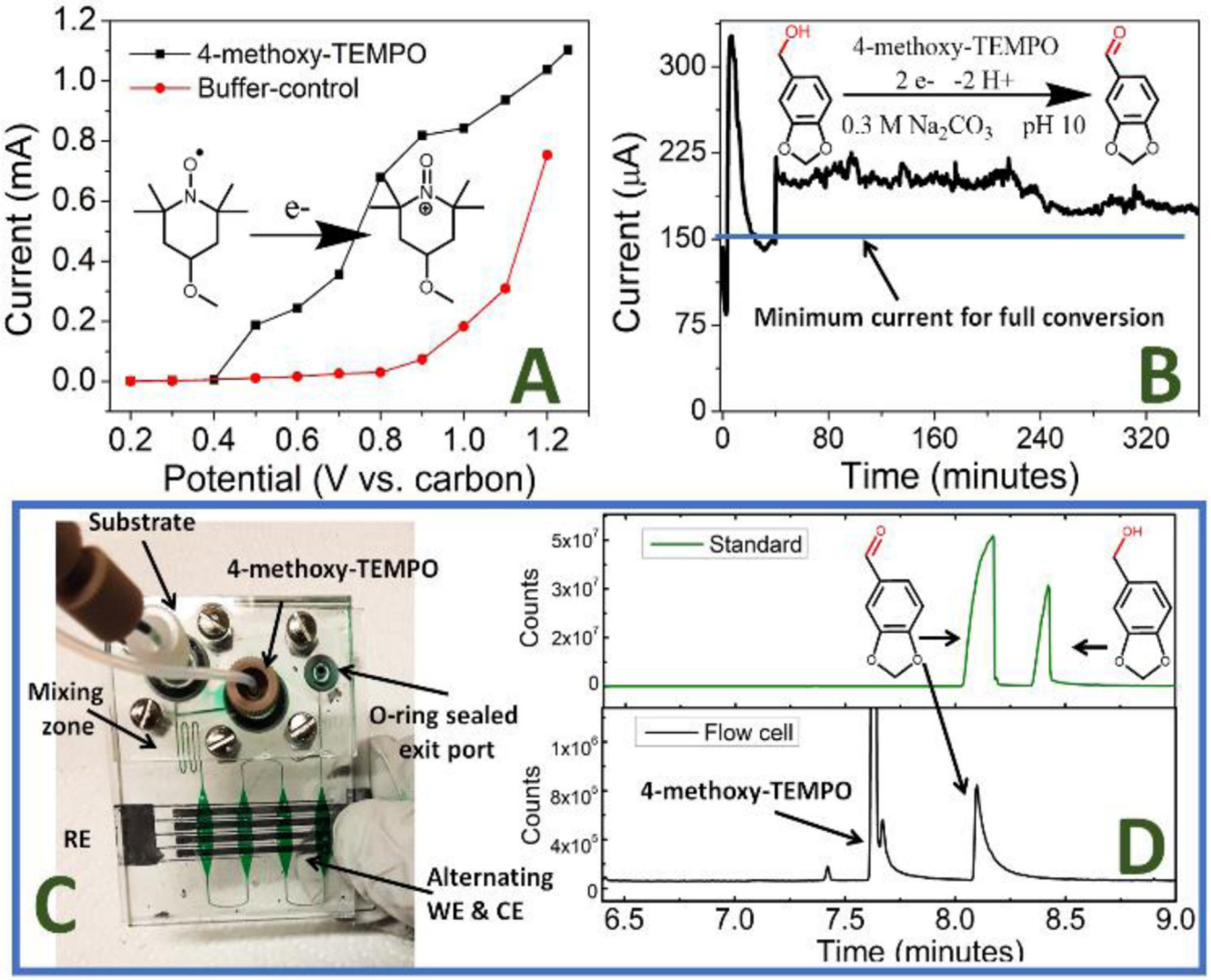

Figure 6.

(A) Electrolysis of TEMPO catalyst and buffer solution in flow without substrate present. (B) Bulk electrolysis of piperonyl aldehyde. (C) Picture of flow cell used for electrolysis (D) GC-MS data of a known solution of piperonal and piperonyl alcohol and post electrolysis products from the oxidation of piperonyl alcohol.